Possible Detection of Cosmological Reionization Sources

M. Stiavelli, S. Michael Fall, and N. Panagia¹

Space Telescope Science Institute, 3700 San Martin Drive, Baltimore, MD 21218

ABSTRACT

We compare the available catalogs of $z \approx 6$ galaxies in the Hubble Ultra-Deep Field (UDF) and in the Great Observatories Origins Deep Survey (GOODS) with the expected properties of the sources of cosmological reionization from our previous theoretical study. Our approach is based on the mean surface brightness of the sources required for reionization and depends on relatively few undetermined parameters. We find that the observed mean surface brightness of galaxies at $z \approx 6$ is sufficient for reionization, provided that the sources are composed of hot metal-free or metal-poor stars, regardless of whether reionization occurs over a short or long interval of redshift. The broad agreement between the new observations and our predictions suggests that we may have detected the sources responsible for some or even all of the reionization of hydrogen.

Subject headings: cosmology: early Universe, observations, theory

1. Introduction

The reionization of the intergalactic medium (IGM) was undoubtedly one of the most significant events in cosmic history. It completely changed the opacity of the universe to ionizing radiation and may also have influenced the formation and evolution of galaxies and other structures (see, e.g., Loeb & Barkana 2002). The absence of strong Gunn-Peterson Ly α absorption in the spectra of distant quasars indicates that reionization was complete by $z\approx 6$ (Becker et al. 2001; Fan et al. 2002; White et al. 2003), while the polarization of the cosmic microwave background (CMB) radiation indicates that it began at higher redshifts (Spergel et al. 2003). A major goal of extragalactic astronomy is to detect and characterize the sources of UV radiation responsible for reionization.

In a previous paper, we outlined a method to guide and interpret searches for the reionization sources with existing and planned telescopes (Stiavelli, Fall, & Panagia 2004,

¹ESA Space Telescope Division

hereafter Paper I). Our work builds on several important papers in this field, including those by Miralda-Escudé & Rees (1998) and Madau, Haardt, & Rees (1999). We consider the same physical processes as previous authors, but we focus on low-metallicity sources (Population II and III stars), which are more efficient ionizers and are perhaps more natural at high redshifts (e.g., Malhotra & Rhoads 2002). We ignore active galactic nuclei (AGN) because constraints from the X-ray background indicate that they make a relatively small contribution to reionization (Dijkstra et al. 2004). We express our results in terms of the mean surface brightness of the reionization sources instead of their volume emissivity or star formation density because this allows a more direct comparison with observations. We focus on the expected location of the sources in a plot of mean surface number density against apparent magnitude. Only a moderately narrow band in this diagram is allowed by the demands of producing enough ionizing radiation but not too many heavy elements (for stellar sources).

We showed that the existing deep surveys with the Hubble Space Telescope (HST), such as the Hubble Deep Fields (HDFs: Williams et al. 2000) and the Great Observatories Origins Deep Survey (GOODS: Giavalisco et al. 2004), do not probe far into the allowed part of this diagram, while future deep surveys with the James Webb Space Telescope (JWST) will do so easily. We also pointed out that there was a reasonable chance of detecting the reionization sources with the then-planned HST Ultra-Deep Field (UDF: Beckwith et al., in preparation). This observing program has now been completed, the data have been released, and several papers have appeared with catalogs of sources (Bouwens et al. 2004; Bunker et al. 2004). Here, we combine the available UDF and GOODS observations with our previous theoretical expectations to search for the reionization sources. Throughout this paper, we adopt values of the cosmological parameter derived from the Wilkinson Microwave Anisotropy Probe (WMAP): $\Omega_{\Lambda} = 0.732$, $\Omega_{m} = 0.268$, $\Omega_{b} = 0.044$, and $H_{0} = 71$ km s⁻¹ Mpc⁻¹ (Spergel et al. 2003)

2. Models

Our general method is applicable to a wide variety of reionization sources. For specific predictions, however, we focus on sources composed either of metal-free stars (hereafter Population III) or metal-poor stars ($10^{-3} \lesssim Z/Z_{\odot} \lesssim 10^{-2}$, hereafter Population II). We approximate the spectral energy distributions of these sources by blackbodies with temperatures of 10^5 K for Population III and 5×10^4 K for Population III. These effective temperatures are most appropriate for stellar populations with top-heavy initial mass functions (IMFs dominated by stars more massive than $\sim 30 M_{\odot}$). Since Population III stars are hotter

than Population II stars, they produce more ionizing photons for a given flux at longer wavelengths. In this sense, Population III stars are also more efficient ionizers than AGNs.

Figure 1 shows the expected cumulative mean surface number density of reionization sources as a function of their apparent AB magnitude in the non-ionizing UV continuum at a rest-frame wavelength of 1400 Å. Here we have assumed that the comoving volume density of the sources is constant over the range of redshifts $5.8 \lesssim z \lesssim 6.7$ spanned by *i*-band dropouts in the UDF and GOODS (see below). The luminosity function of the sources is assumed to have the Schechter form, parameterized by its knee M_* and slope α . For reference, the Lyman-break galaxies at z=3 have $M_{*,1400}=-21.2$ and $\alpha=1.6$. (Steidel et al. 1999; Yan et al. 2002). These are the parameters adopted for the top panels of Figure 1. The middle panels have a brighter knee ($M_{*,1400}=-23.2$), and the bottom panels have a steeper slope ($\alpha=1.9$). The predictions in the left panels are for Population III stars; those in the right panels are for Population II stars. (Figure 1 here is a rearrangement of several panels in Figures 2 and 3 of Paper I.)

The requirement that the sources be able to ionize all the hydrogen in the IGM corresponds, for a given spectral shape, to a definite mean surface brightness at any chosen wavelength ($\lambda_{\text{rest}} = 1400 \text{ Å}$ in all cases considered here). This surface brightness depends on the fraction f_c of Lyman-continuum photons that escape from the sources and on the clumpiness C of the IGM, which in turn determines the recombination rate. The surface brightness required for reionization fixes the normalization of the curves in Figure 1, which are labeled by the corresponding parameters (f_c , C). We have calculated these curves from the equation of ionization balance, including both H and He, and the effect of recombinations (as described in detail in Paper I).

The minimum mean surface brightness of the reionization sources is given by $(f_c, C) = (1,1)$; in this case, all Lyman-continuum photons escape and the recombination rate is minimum. For stellar sources, there is also a maximum mean surface brightness, given by the condition that they not produce too many heavy elements. We adopt the generous but non-rigorous limit $Z \lesssim 0.01Z_{\odot}$ on the cosmic mean metallicity (the mean density of heavy elements in stars and interstellar and intergalactic matter divided by the mean baryon density) at z = 6 (explained in detail in Paper I). The shaded regions in Figure 1 are excluded by these constraints, while the clear regions are allowed.

The specific predictions shown in Figure 1 assume that reionization is complete at z=6. This is supported strongly by the Ly α absorption of $z\sim 6$ quasars and by a variety of theoretical arguments and hydrodynamical simulations (Haiman & Holder 2003; Gnedin 2004). The mean surface brightness required for reionization also depends on the interval of redshift over which the sources are active. Here we concentrate on the interval $\Delta z\approx 1$ just

above $z \approx 6$. This closely matches the interval spanned by *i*-band dropouts and is marginally compatible (at 2σ confidence) with the measured CMB polarization (Spergel et al. 2003). The interval $\Delta z \approx 1$ is also likely a worst-case (i.e., minimum-surface-brightness) scenario in the sense that there could be additional reionization sources at redshifts above $z \approx 7$, which would relax the requirements on those below. However, the dependence of the mean surface brightness required for reionization on the redshift interval is relatively weak, increasing by only 0.1, 0.4, and 0.8 magnitudes as Δz increases from 1 to 3, 1 to 10, and 1 to 30 (for $C \approx 1$).

3. Observations

We now compare the predictions of Paper I, summarized in the previous section, with recent observations from the UDF and GOODS. The UDF observations were made in 400 orbits on a single pointing with the wide-field channel (WFC) of the Advanced Camera for Surveys (ACS). The two longest integrations, 144 orbits each, were made in the *i*-band (F775W filter) and *z*-band (F850LP filter). We base our analysis on the *i*-band dropouts ($z \approx 6$ galaxies) identified by Bunker et al. (2004) using the Sextractor program (Bertin & Arnouts 1996) in the final combined images. The magnitudes and colors of the objects were measured in apertures 0.5 arcsec in diameter. The UDF catalog includes 53 objects with $i-z \geq 1.3$ and 22 with $i-z \geq 2.0$ down to a limiting magnitude of z=28.5 at S/N=8, where the incompleteness is only 2% (Table 1 of Bunker et al. 2004). We analyze the $i-z \geq 1.3$ and $i-z \geq 2.0$ subsamples separately. The latter may miss some high-reshift objects, but it should be nearly free of contamination by low-redshift objects. We have verified that the same selection criteria produce essentially the same samples of objects when applied to the *z*-detected catalog released by the UDF team (Beckwith et al., in preparation).

We combine these UDF observations with wider and shallower, but otherwise similar, observations from GOODS to obtain more reliable estimates of the bright part of the surface density-magnitude relation. For consistency with the UDF catalog, we again use magnitudes and colors measured in apertures 0.5 arcsec in diameter, taken from the V1.0 GOODS catalog (Dickinson et al. 2004; Giavalisco et al., in preparation). This includes 77 objects with $i-z \geq 1.3$ and 14 with $i-z \geq 2.0$ down to a limiting magnitude of z=26.8 at S/N=10. We correct these counts for incompleteness, which increases from 10% at z=26.0 to 40% at z=26.5 for compact sources. We use the GOODS observations brighter than z=26.5 and the UDF observations fainter than this magnitude. The expected uncertainties in the surface density due to Poisson fluctuations alone range from 60% at z=24 to 20% at z=28, while

those due to large-scale structure range from 20% to 40% at the same magnitudes (Somerville et al. 2004; Bunker et al. 2004). We do not correct the observed mean surface brightness for objects fainter than our detection limits in luminosity and/or surface brightness. In this sense, all our empirical estimates are lower limits to the true mean surface brightness.

Before comparing these observations with our predictions, we must examine the relation between the measured z-band magnitudes and the rest-frame 1400 Å magnitudes adopted in Figure 1. We estimate the offset between these magnitudes by convolving the total z-band response function with 10^5 K and 5×10^4 K black-body spectra truncated below rest-frame 1216 Å and redshifted through the interval 5.8 < z < 6.7. This procedure mimics observations of reionization sources composed of Population III and Population II stars with heavy HI absorption by some combination of stellar, interstellar, or intergalactic material. The resulting offsets between the z-band and rest-frame 1400 Å magnitudes are -0.03 mag for Population III sources and +0.02 mag for Population II sources. Such small offsets are the product of a fortuitous near-cancellation. Sources at $z \approx 5.8$ appear brighter in the z-band (by few tenths of a magnitude) than at rest-frame 1400 Å because their blue UV continua are measured at shorter wavelengths, which contributes a negative correction. However, objects at $z \approx 6.7$ appear fainter than at rest-frame 1400 Å because the z-band samples mostly the part of the spectrum attenuated by HI, which contributes a positive correction. Thus, for a uniform distribution of redshifts within the interval $5.8 \lesssim z \lesssim 6.7$, the offsets from the two extremes tend to cancel out. Given these small differences between the z-band and rest-frame 1400 Å magnitudes, we simply ignore them in the following.

The resulting cumulative surface density-magnitude relation is shown by the stepped lines in each panel of Figure 1. The upper (light-gray) line refers to the $i-z \geq 1.3$ color cut, while the lower (dark-gray) line refers to the more stringent $i-z \geq 2.0$ color cut. We expect the true relation to lie between the two stepped lines. Both of these relations appear generally compatible with our predictions, especially when allowance is made for the large statistical uncertainties at the bright ends. The observed relation extends into the shaded region at the bright end, but we have checked that this does not violate the global metallicity constraint, which pertains to the mean surface brightness when integrated over all magnitudes. We find that the integrated surface brightness of the objects brighter than our limiting magnitude $(z_{\text{lim}} = 28.5)$ is $\mu_{AB} = 25.4$ and 26.7 mag arcmin⁻², respectively, for the $i-z \geq 1.3$ and $i-z \geq 2.0$ subsamples. These are consistent with our predicted minimum surface brightness, $\mu_{AB} = 28.8$ and 27.2 mag arcmin⁻², for reionization by Population III and Population II sources, respectively, and a redshift interval $\Delta z = 1$ (Paper I). We have repeated the entire analysis above with the objects selected by the same criteria from the catalog released by the UDF team and obtained the same values of the mean surface brightness to within 10%.

4. Comparisons

Our conclusion about the ability of the sources detected in the UDF to reionize the IGM differs from the one reached by Bunker et al. (2004). The reason for this is that the two studies, which are based on the same observations, adopt different conditions for reionization; ours is taken from Paper I, theirs from equation (27) of Madau et al. (1999). These conditions involve different assumptions about the temperature $T_{\rm IGM}$ of the IGM and the ionizing efficiencies of the sources as given by the ratio $\epsilon_{\rm ion} \equiv \dot{N}_{\rm ion}/(\nu L_{\nu})_{1400}$ of the production rate of ionizing photons to the luminosity in the non-ionizing UV continuum at 1400 Å, which depends on the effective temperature and hence the metallicity and IMF of a stellar population (Baraffe & El Eid 1991; Tumlinson & Shull 2000; Bromm, Kudritzki, & Loeb 2001; Schaerer 2003). As in Paper I, we adopt $T_{\rm IGM}=20,000~{\rm K}$ and $\epsilon_{\rm ion}=2\times10^{11}$ erg⁻¹ (Population III) or $\epsilon_{\text{ion}} = 4.4 \times 10^{10} \text{ erg}^{-1}$ (Population II), while Madau et al. (1999) adopt $T_{\rm IGM} = 10,000 \text{ K}$ and $\epsilon_{\rm ion} \approx 7 \times 10^9 \text{ erg}^{-1}$ (Population I, with solar metallicity and a Salpeter IMF). Apart from these differences, the two conditions are almost identical (within $\sim 10\%$), as we have verified by test calculations with the same values of $T_{\rm IGM}$, $\epsilon_{\rm ion}$, f_c , and C. The ionization conditions are, however, expressed differently: ours in terms of a surface brightness, theirs in terms of a volume emissivity or star formation density.

The temperature of the IGM and the metallicity and IMF of the stellar population can each change the mean surface brightness required for reionization by factors of a few. The recombination coefficient and hence the required ionization rate is a factor of 2 lower for $T_{\rm IGM} = 20,000 \text{ K}$ than for $T_{\rm IGM} = 10,000 \text{ K}$. The higher IGM temperature seems more appropriate for several reasons. The equilibrium temperature of metal-poor HII regions excited by hot stars is $\sim 20,000$ K (see, e.g., Osterbrock 1989). This is also close to the inferred temperature of the IGM at 2 $\lesssim z \lesssim$ 4 (Zaldarriaga, Hui, & Tegmark 2001). In the simplest non-equilibrium models (those with little or no late heating), the IGM cools following reionization, and has $T_{\rm IGM} \gtrsim 20,000$ K at $z \approx 6$ (Theuns et al. 2002; Hui & Haiman 2003). The ionizing efficiency of a stellar population increases by a factor of 3 for a Salpeter IMF and a factor of 10 for a top-heavy IMF as the metallicity decreases from solar to zero metallicity (Schaerer 2003). The mean metallicity, averaged over all galaxies, is roughly solar in the present-day universe and must have been lower at the epoch of reionization, although we do not know by exactly how much. The ionizing efficiency of a stellar population also depends on the IMF, increasing by factors of 3 (for solar metallicity) to 10 (for zero metallicity) between a Salpeter IMF and a top-heavy IMF (Bruzual & Charlot 2003; Schaerer 2003). The latter is favored by recent theoretical studies of primordial star formation (e.g., Abel, Bryan, & Norman 2000; Bromm, Coppi, & Larson 2002).

The shortfall of ionizing photons estimated by Bunker et al. (2004) using the Madau et

al. (1999) condition is at least a factor of 3. The different assumptions we have made about the IGM temperature, stellar metallicity, and IMF each reduce the mean surface brightness required for reionization by factors of 2, 3-10, and 3-10, respectively. Any two of these factors would be enough to satisfy the reionization condition and all three taken together (as we have assumed in Paper I) do so with a comfortable margin.

5. Conclusions

Our main conclusion is that the surface brightness-magnitude relation for $z \approx 6$ objects detected in the UDF and GOODS agrees remarkably well with our predicted relation for metal-poor reionization sources. In particular, the observed integrated surface brightness is consistent with that required for reionization with reasonable values of the escape fraction $(0.05 < f_c < 0.5)$ and clumpiness parameter (1 < C < 30) if the sources are composed either of Population III or Population II stars with a top-heavy IMF. Reionization by sources with a Salpeter IMF, although possible, is more difficult, requiring both a high escape fraction and a very low metallicity.

We find that the shape of the observed surface brightness-magnitude relation at $z \approx 6$ is roughly similar to that of the Lyman-break galaxies at $z \approx 3$ (consistent with the conclusions of Bouwens et al. 2004 and Bunker et al. 2004). However, we obtain somewhat better agreement if the luminosity function of the $z \approx 6$ galaxies has a brighter knee and a steeper slope. It is worth noting that, as the slope approaches the divergence value $\alpha = 2$, progressively more of the ionizing radiation comes from fainter, possibly undetected sources. Population II sources require higher values of f_c and lower values of C than Population III sources, because cooler stars are less efficient ionizers. It is not clear, however, whether sufficiently high values of f_c could be reached in sources that were already enriched in metals and dust and therefore likely to have more UV absorption.

The predictions presented here are based on the assumption that reionization occurs over the relatively small interval of redshift $\Delta z \approx 1$ just above $z \approx 6$. It is remarkable that, even in this most demanding case, the observed objects are sufficient to reionize the IGM. Of course, it is possible that reionization began much earlier. The polarization of the CMB measured by WMAP indicates that the IGM was at least partly ionized at $z \sim 20$ (albeit with large uncertainties, Spergel et al. 2003). However, the high temperature of the IGM at $z \approx 4$ inferred from quasar absorption-line systems indicates that much of the heating accompanying reionization occurred at z << 20 (Theuns et al. 2002; Hui & Haiman 2003). Some theoretical models suggest that reionization might have occurred more than once, for example at $z \approx 15$ and then again at $z \approx 6$ (Cen. 2003). We conclude that, even if the

 $z \approx 6$ objects observed in the UDF and GOODS were not the only sources responsible for the reionization of the IGM, they would have contributed substantially to its final stages.

An important future development will be to extend of this analysis to observations at infrared wavelengths. In this way, we could attempt to detect additional reionization sources at redshifts beyond $z \approx 7$ and to determine their contribution relative to the sources at lower redshift discussed here. Such observations in and near the UDF have already been made with the Near Infrared Camera and Multi-Object Spectrometer (NICMOS) on HST and will become available soon (Thompson et al., in preparation). Further progress could be made with the Wide Field Camera 3 if and when it is installed on HST. However, a complete census of all the reionization sources, especially any at $z \gtrsim 12$, must await the launch of JWST.

We are grateful to the UDF and GOODS teams for obtaining and releasing the data on which this study is based. We also thank Daniel Schaerer for making his stellar population models available to us in electronic form. *HST* data are obtained at STScI, which is operated by AURA, Inc., under NASA contract NAS5-26555. This work is partially supported by NASA Grant NAG5-12458.

REFERENCES

Abel, T., Bryan, G. L., & Norman, M. L. 2000, ApJ, 540, 39

Baraffe, I., & El Eid, M. F. 1991, A&A, 245, 548

Becker, R. H., et al. 2001, AJ, 122, 2850

Bertin, E., & Arnouts, S. 1996, A&AS, 117, 393

Bouwens, R. J., Illingworth, G. D., Thompson, R. I., Blakesless, J. P., Dickinson, M. E., Broadhurst, T. J., Eisenstein, D. J., Fan, X., Franx, M., Meurer, G., & van Dokkum, P. 2004, ApJ, 606, L25

Bromm, V., Coppi, P. S., & Larson, R. B. 2002, ApJ, 564, 23

Bromm, V., Kudritzki, R. P., & Loeb, A. 2001 ApJ, 552, 464

Bruzual, G., & Charlot, S. 2003, MNRAS, 344, 1000

Bunker, A. J., Stanway, E. R., Ellis, R. S., & McMahon, R. G. 2004, MNRAS, submitted (astro-ph/0403223)

Cen, R. 2003, ApJ, 591, 12

Dickinson, M., et al. 2004, ApJ, 600, L99

Dijkstra, M., Haiman, Z., & Loeb, A. 2004, ApJ, submitted (astro-ph/0403078)

Fan, X., et al. 2002, AJ, 123, 1247

Giavalisco, M., et al. 2004, ApJ, 600, L93

Gnedin, N. Y. 2004, ApJ, in press (astro-ph/0403699)

Haiman, Z., & Holder, G. P. 2003, ApJ, 595, 1

Hui, L., & Haiman, Z. 2003, ApJ, 596, 9

Loeb, A., & Barkana, R. 2002, ARAA, 39, 19

Madau, P., Haardt, F., & Rees, M. J. 1999, ApJ, 514, 648

Malhotra, S., & Rhoads, J. E. 2002, ApJ, 565, L71

Miralda-Escudé, J., & Rees, M.J. 1998, ApJ, 497, 21

Osterbrock, D.E. 1989, Astrophysics of Gaseous Nebulae and Active Galactic Nuclei, (Mill Valley: Univ. Science Books)

Schaerer, D. 2003, A&A, 397, 527

Somerville, R. S., Lee, L., Ferguson, H. C., Gardner, J. P., Moustakas, L. A., & Giavalisco, M. 2004, ApJ, 600, L171

Spergel, D. N., et al. 2003, ApJS, 148, 175

Steidel, C. C., Adelberger, K. L, Giavalisco, M., Dickinson, M., & Pettini, M. 1999, ApJ, 519, 1

Stiavelli, M., Fall, S. M., & Panagia, N. 2004, ApJ, 600, 508

Theuns, T., Schaye, J., Zaroubi, S., Kim, T.-S., Tzanavaris, P., & Carswell, B. 2002, ApJ, 567, L103

Tumlinson, J., & Shull, J. M. 2000, ApJ, 528, L65

White, R. L., Becker, R. H., Fan, X., & Strauss, M. A. 2003, AJ, 126, 1

Williams, R., et al. 2000, AJ, 120, 2735

Yan, H., Windhorst, R. A., Odewahn, S. C., & Cohen, S. H. 2002, ApJ, 580, 725

Zaldarriaga, M., Hui, L., & Tegmark, M. 2001 ApJ, 557, 519

This preprint was prepared with the AAS LATEX macros v5.2.

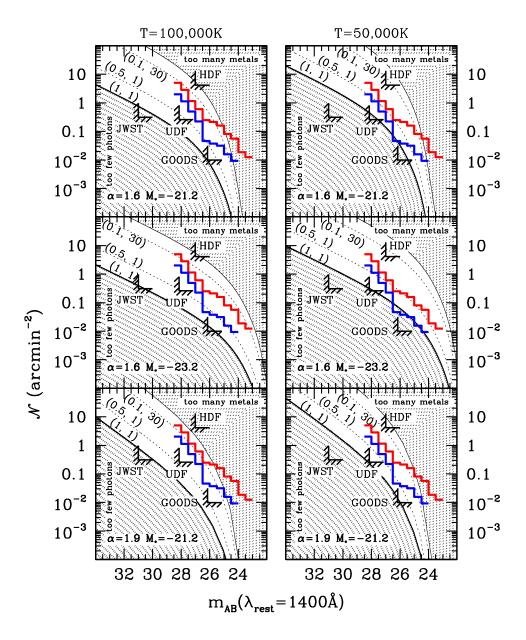


Fig. 1.— Cumulative mean surface number density vs apparent rest-frame 1400Å AB magnitude of reionization sources with different luminosity functions and effective temperatures. In each panel, the lower solid line represents the minimum-surface brightness model, with $(f_c, C) = (1, 1)$, while the upper thin solid line represents the global metallicity constraint. The thin dotted lines correspond to models with $(f_c, C) = (0.5, 1)$ and (0.1, 30). The thick stepped lines represent the observations from the UDF and GOODS with the two color cuts: $i - z \ge 1.3$ (light gray) and $i - z \ge 2.0$ (dark gray). The L-shaped markers delimit the areas probed by GOODS, HDF, UDF, and an ultra-deep survey with JWST. The adopted parameters of the luminosity function are indicated in each panel. The left and right panels refer to sources composed, respectively, of Population III and II stars with a top-heavy IMF.